ELSEVIER

Journal of Molecular Catalysis A: Chemical 130 (1998) 177–185

JOURNAL OF MOLECULAR CATALYSIS A: CHEMICAL

Study of the catalyst deactivation in the base-catalyzed oligomerization of acetone

Juana I. Di Cosimo, Carlos R. Apesteguía *

Instituto de Investigaciones en Catálisis y Petroquímica (INCAPE), UNL-CONICET, Santiago del Estero 2654, 3000 Santa Fe, Argentina

Received 2 May 1997; accepted 10 September 1997

Abstract

The deactivation of unpromoted MgO and alkali-promoted MgO catalysts in the vapor-phase self-condensation of acetone was studied. The reaction was catalyzed by basic sites and major products were mesityl oxide, isomesityl oxide and isophorone. Catalysts deactivated because of coke formation. Both the initial catalyst deactivation (d_0, h^{-1}) and the product distribution depended on contact time (W/F^0): d_0, and the selectivity to mesityl oxide increased when W/F^0 was increased. It is proposed that non-cyclic trimers, such as phorone, which are produced by aldol condensation of mesityl oxide with acetone, are the key intermediate species for coke formation. These non-cyclic trimers are highly unsaturated compounds that remain strongly bound to the catalyst surface yielding higher non-volatile oligomeric compounds which block basic active sites. Promotion of MgO with alkaline metal ions increased the d_0 value measured on unpromoted MgO following the sequence Li < Na < K < Cs: the stronger the promoter oxide basicity, the higher the catalyst deactivation. Enhancement of the MgO basicity by alkali addition strengthens the interaction between the solid surface and non-cyclic trimers, and improves the catalyst ability for abstracting the α-proton from the acetone molecule. As a consequence, the aldol condensation synthesis of tetramers and heavier polymers is favored which results in an increasing coke formation.

Keywords: Catalyst deactivation; Base catalysis; Acetone oligomerization; MgO-based catalysts

1. Introduction

Lately, increasing research efforts have been devoted to the use of basic solids in heterogeneous catalysis. Solid base catalysts are desirable for several reasons. They permit base catalyzed reactions in the vapor phase. Combination of strong electric fields and geometrical constraints allows optimisation of product selectivity and conversion. In liquid-phase reactions the catalyst can be separated from the reaction solving the problem of disposing of concentrated basic solutions. Unfortunately, solid bases are often rapidly deactivated either by the presence of acid molecules and water in gas phase or by in situ coke formation through secondary side reactions. This limitation has traditionally thwarted the potential of solid bases to replace environmentally problematic and corrosive liquid bases. In spite of this, and in sharp contrast to the extensive research on solid acids deactivation, few investigations have been focused on the deactivation of solid bases at reaction condi-

* Corresponding author. Tel.: +54-42-555279; fax: +54-42-531068/553727; e-mail: capesteg@fiqus.unl.edu.ar

1381-1169/98/$19.00
PII S1381-1169(97)00204-5

tions. It is therefore of both fundamental and practical interest to undertake studies regarding deactivation of solid catalysts in base-catalyzed reactions.

Alkaline earth metal oxides are reported to be active and selective in a variety of organic reactions involving formation of carbanion intermediates such as alkene isomerization, Cannizzaro and Tischenko reactions, Michael, Wittig and Knoevenagel condensations, etc. [1,2]. One of the most thoroughly investigated alkaline-earth oxides is magnesium oxide which is usually regarded as a typical strong solid base catalyst. The use of pure and promoted MgO catalysts in oxidative coupling of methane [3,4], 1-butene isomerization [5], and synthesis of organic chemicals by either self- [6,7] or cross-condensation reactions [8,9] has been extensively documented. In recent work [10], we have shown that magnesium oxide promoted with group IA or IIA metals readily catalyzes the synthesis of valuable α,β-unsaturated ketones, such as mesityl oxide and isophorone, from the vapor-phase aldol condensation of acetone.

In this paper we have studied the deactivation of unpromoted and alkali-promoted magnesium oxides in the gas-phase oligomerization of acetone. Our objectives were twofold: first, to identify the species responsible for the catalyst activity decay; and second, to relate the concerted and sequential pathways required in the deactivating mechanism with the acid–base properties of the catalyst surface.

2. Experimental

2.1. Catalyst preparation and characterization

Magnesium oxide was prepared by adding 250 ml of distilled water to 25 g of commercial MgO (Carlo Erba, 99%, 27 m^2/g of surface area) at room temperature in a stirred glass reactor. Temperature was then raised to 353 K and stirring was maintained for 4 h. Sample was dried in an oven at 358 K overnight. The obtained $Mg(OH)_2$ was thermally decomposed in N_2 at 30 ml/min (STP). Sample was first treated at 623 K for 2 h, then heated to 773 K and finally maintained at this temperature for 8 h. Typical surface areas of the resulting magnesium oxide were between 110–150 m^2/g.

A series of alkali-promoted MgO catalysts were prepared as described previously [10]. About 1 wt% of the promoter was added to MgO by incipient wetness impregnation using nitrate or hydroxide solutions containing the appropriate amount of the alkaline metal ions. The impregnated samples were dried and then thermally decomposed following the same procedure described above for the preparation of MgO. The alkali-promoted MgO samples are identified here as A/MgO, A being Li, Na, K, or Cs.

The chemical composition of A/MgO samples was analyzed by atomic absorption spectrometry (AAS). BET surface areas (S_g) were determined by nitrogen adsorption at 77 K using a Micromeritics Accusorb 2100 E sorptometer. The chemical composition and the surface area of the catalysts are presented in Table 1. The crystalline phase composition of calcined MgO and A/MgO samples was characterized by X-ray diffraction (XRD) with a Rich-Seifert Iso Debiflex 2002 diffractometer, using nickel filtered CuKα radiation.

2.2. Carbon dioxide chemisorption

Carbon dioxide chemisorption was performed in a conventional glass vacuum apparatus equipped with an MKS Baraton pressure gauge. Catalysts were outgassed at 773 K in a vacuum of 2.10^{-6} kPa. The pressure range of isotherms was 0–35 kPa. After cooling to room temperature a first isotherm was drawn for measuring the total CO_2 uptake. Then, and after 1 h of evacuation at room temperature, a second isotherm was performed to determine the amount of weakly adsorbed CO_2. The amount of irreversibly held CO_2 was calculated as the difference between total and weakly adsorbed CO_2.

2.3. Catalytic testing

Vapor-phase aldol condensation of acetone was performed at 573 K and 100 kPa in a flow system with a fixed-bed reactor [11]. Care was taken to avoid diffusional limitations. Prior to catalytic tests, the samples were pretreated in nitrogen at 773 K for 1 h to remove water and carbon dioxide. Typical catalyst loading was 200 mg. Standard catalytic tests were carried out at a contact time (W/F^0) of 49 g catalyst h/mol of acetone. Acetone was delivered by a syringe pump and vaporised in a flow of hydrogen with a H_2/acetone molar ratio of 12 before entering the reaction zone. Acetone conversion was always lower than 20%. The reaction products were analyzed by on-line gas chromatography using a Varian Star 3400 CX chromatograph equipped with flame ionisation detector and a 20% SP-2100/0.1% Carbowax 1500 on 100/120 Supelcoport column. Data were collected every 30 min for 10 h. Main reaction products were mesityl oxide (MO), isomesityl oxide (IMO) and isophorone (IP); trace amounts of diacetone alcohol (DAA), phorones, mesitylene and light hydrocarbons were also detected. Selectivities (S_i) were calculated on a carbon atom basis.

3. Results

3.1. Catalyst characterization

The BET surface areas of MgO and A/MgO samples are presented in Table 1. It is shown that the MgO surface area diminished upon addition of the alkaline metal ions. The crystalline phase composition of the samples was characterized by X-ray diffraction technique. In all cases only the MgO periclase phase (ASTM 4-0829) was detected.

The number of available basic sites was determined by CO_2 chemisorption. Langmuir-type adsorption isotherms were obtained in all cases. The values of n_i, the number of moles of irreversibly held CO_2 per square meter at saturation, were obtained from the isotherm plateau, at $P = 20$ kPa. Results are given in Table 1. The number of basic sites on unpromoted MgO was $n_i = 2.16$ μmol/m^2. Promotion of MgO with group IA metals increased the number of surface basic sites. The highest n_i value ($n_i =$ 4.60 μmol CO_2/m^2) corresponded to the Li/MgO sample. In order to quantify the specific effect that the addition of promoter A has on the CO_2 adsorption capacity of the MgO sample, the chemisorption data should be re-

Table 1
Catalyst characterization: chemical composition, BET surface areas, CO_2 uptakes and initial reaction rates

Catalyst A/MgO	Alkali A loading		Oxygen partial charge in A_xO	S_g (m^2/g)	CO_2 chemisorption		r_0 (μmol/m^2)
	(wt%)	n_A (μmol/m^2)	q_0^a		n_i (μmol/m^2)	M^b (mol CO_2/mol A)	
MgO	0.00	0.00	0.50	119	2.16	0.00	24
Li/MgO	1.04	18.50	0.80	81	4.60	0.13	36
Na/MgO	0.92	4.13	0.81	97	3.35	0.28	31
K/MgO	0.88	2.12	0.89	106	2.78	0.30	27
Cs/MgO	0.84	0.62	0.94	102	2.50	0.55	26

[a] From Ref. [17].
[b] See text for definition of parameter M.

lated to the unit molar content of the promoter. Thus, we have defined the parameter $M = \Delta n_i / n_A$, where Δn_i (mol CO_2/m^2) is the difference between the number of moles of CO_2 irreversibly adsorbed per square meter on A/MgO and on unpromoted MgO, and n_A (mol A/m^2) is the amount of moles of promoter A contained per square meter in the corresponding A/MgO sample. The value of parameter M (mol CO_2/mol A) is therefore a measure of the effect the addition of 1 mol of A has on increasing the CO_2 adsorption capacity of the MgO sample. The n_A and M values are reported in Table 1.

The catalyst activity was determined by measuring the initial reaction rate (r_0, μmol acetone/h m^2) at $T = 573$ K and $W/F^0 = 49$ g catalyst h/mol acetone. Because the acetone conversion diminished with time-on-stream, the r_0 values were calculated by extrapolating the log r_0 vs t plots to zero time (Fig. 1). Promotion with alkaline metal ions activated the MgO catalyst and in all the cases the r_0 values corresponding to A/MgO samples were higher than that measured on unpromoted MgO (Table 1). The initial activity of A/MgO samples was in the order Li > Na > K > Cs, which is similar to that followed by the concentration of basic centers on the samples as determined by CO_2 chemisorption (n_i values, column 6, Table 1). Actually, the plot of r_0 as a function of n_i is a straight line (the plot is not shown here).

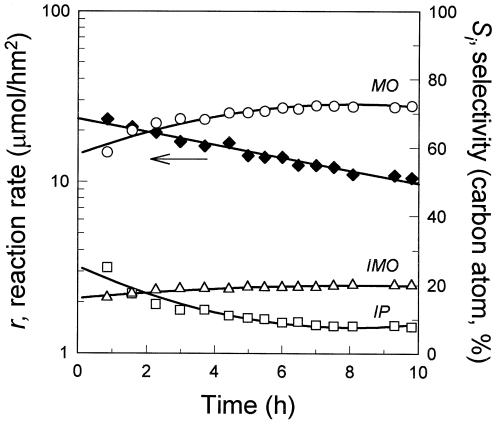

Fig. 1. Time dependence of acetone oligomerization over unpromoted MgO ($T = 573$ K, $P = 100$ kPa, $W/F^0 = 49$ g catalyst h/mol).

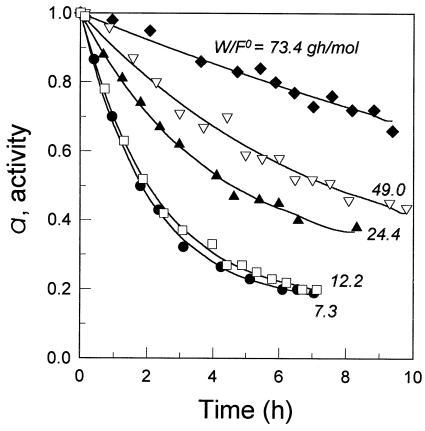

Fig. 2. Acetone oligomerization activity (a) as a function of time and W/F^0 over unpromoted MgO ($T = 573$ K, $P = 100$ kPa).

3.2. Deactivation of unpromoted MgO

Fig. 1 illustrates the time-on-stream behavior of unpromoted MgO during the self-condensation of acetone at $W/F^0 = 49$ g catalyst h/mol of acetone. The reaction rate diminished as a function of time and the catalyst lost about 50% of its initial activity after the 10 h run due to a slow but progressive deactivation process. The selectivities to the major products, e.g., mesityl oxide, isomesityl oxide, and isophorone, remained essentially stable after the first 3 h of time-on-stream.

To obtain insight on the species responsible for catalyst deactivation, additional catalytic tests at different contact times, between 7.3 and 73 g h/mol, were carried out. The curves representing the MgO activity decay as a function of time and W/F^0 are shown in Fig. 2. The activity is defined as $a_{(t)} = r_t/r_0$, where r_t and r_0 are the reaction rates at time t and zero time, respectively. Fig. 2 shows that the catalyst activity decay diminishes with increasing W/F^0. To quantitatively evaluate the effect that varying W/F^0 has on catalyst deactivation we deter-

mined the initial catalyst deactivation (d_0, h^{-1}) by measuring the initial slopes, $-(da/dt)_{t=0} = d_0$ of the activity versus time curves shown in Fig. 2. The obtained d_0 values are represented as a function of W/F^0 in Fig. 3. The d_0 value increased from 0.04 h^{-1} at $W/F^0 = 73$ g h/mol to 0.41 h^{-1} at $W/F^0 = 7.3$ g h/mol. In Fig. 3 we also plotted the values of the initial selectivities toward MO and IP as a function of contact time. It is shown that the selectivity to IP increases at the expense of MO when W/F^0 is increased. The IMO selectivity remained essentially constant (S_{IMO} = ca. 20%) in the W/F^0 range studied. The selectivity toward phorone was always lower than 2%.

3.3. Deactivation of alkali-promoted MgO samples

Similarly to unpromoted magnesium oxide, the alkali-promoted MgO samples exhibited a loss of activity along the catalytic test. The curves representing the activity decay as a function of time at $W/F^0 = 49$ g catalyst h/mol acetone are given in Fig. 4. It is shown that alkali-promoted MgO samples deactivated faster than unpromoted MgO, following the order Li < Na < K < Cs. From the initial slopes of the a vs t curves of Fig. 4, we determined the d_0 values. On Cs/MgO sample we obtained $d_0 = 0.52$ h^{-1}, a value about five times higher than that measured on pure MgO ($d_0 = 0.11$ h^{-1}). In an attempt to relate catalyst deactivation with the basic properties of the samples, we plotted the d_0 values determined from Fig. 4 against the values of parameter M of Table 1. As it is shown in Fig. 5, a linear correlation between d_0 and M was obtained.

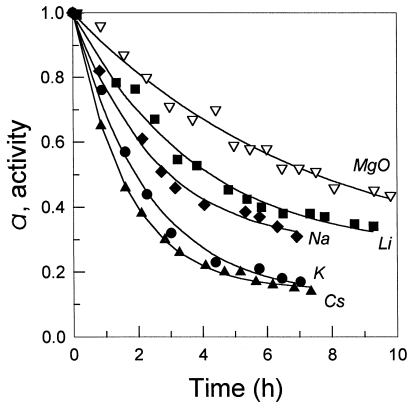

Fig. 4. Acetone oligomerization activity (a) as a function of time over alkali-promoted MgO catalysts ($T = 573$ K, $P = 100$ kPa, $W/F^0 = 49$ g catalyst h/mol).

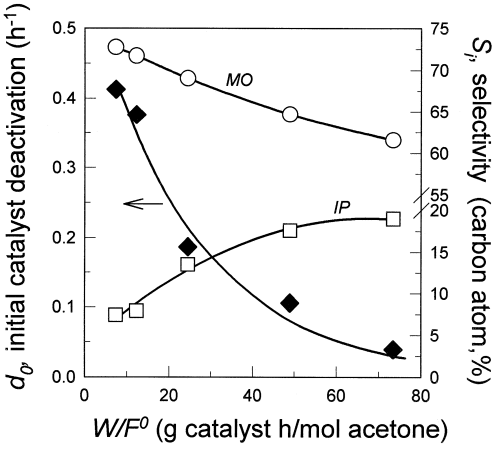

Fig. 3. Initial catalyst deactivation (d_0) and selectivity for the self-condensation of acetone as a function of contact time over unpromoted MgO ($T = 573$ K, $P = 100$ kPa).

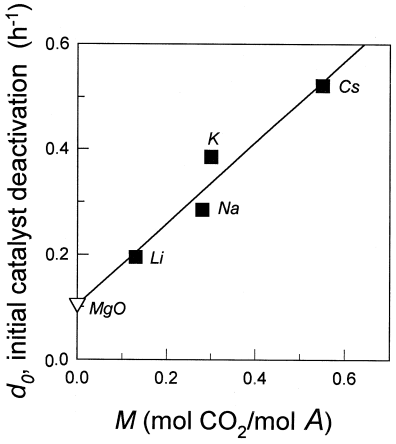

Fig. 5. Initial catalyst deactivation as a function of the specific increase of the irreversible adsorption of CO_2 on A/MgO samples (M).

4. Discussion

4.1. Reaction network and base catalysis

The aldol condensation of acetone produces initially diacetone alcohol which dehydrates to yield MO. We detected only traces of DAA even when low contact times were employed, thereby indicating that on MgO and under our experimental conditions DAA was an unstable intermediate which rapidly decomposed after formation. Production of numerous compounds is then possible through a complex reaction network which involves self- and cross-condensations between the MO itself or with the acetone. Fig. 6 shows a simplified scheme of the multi-step sequence proposed by several authors [10,12–14] for interpreting the synthesis of isophorone from the acetone oligomerization over basic catalysts. Major reaction products are α,β-unsaturated carbonyl compounds which are typical products of Knoevenagel-like reactions. Nevertheless, the oligomerization of acetone can also proceed through acid catalysis producing mainly hydrocarbons. In fact, over acid catalysts isobutene and acetic acid are obtained by cracking of DAA whereas mesitylene is formed via an internal 2,7-aldol condensation of 4,6-dimethylhepta-3,5-dien-2-one which in turn is obtained by aldol condensation of MO with a deprotonated acetone molecule [13,15,16]. In the present paper, the absence of isobutene, acetic acid and mesitylene among the reaction products suggests that the oligomerizaton of acetone over our MgO-based samples is essentially catalyzed by surface basic sites. We arrived to a similar conclusion in a previous work by performing in situ poisoning experiments [10]. By doping the acetone with acetic acid or pyridine, we observed that the magnesium oxide activity is suppressed by co-feeding acetic acid along with acetone but is almost unaffected by the presence of pyridine. Furthermore, a linear correlation is observed in Table 1 between the reaction rate and the concentration of basic sites on the sample as determined by carbon dioxide chemisorption. This proportionality between r_0 and n_i provides additional support for the interpretation that the reaction is effectively controlled by the surface base property. The function of the base is to abstract from the acetone molecule the proton in α position (H^{α}) to the carbonyl group, involving formation of a carbanion intermediate which is stabilised by the enolate resonance isomer. The carbanion then reacts with the carbonyl group of a second acetone molecule to give DAA and, subsequently, MO. Our results of Table 1 and Fig. 1 show that magnesia is active for the vapor-phase acetone condensation reaction, thereby indicating that it contains basic sites strong enough to abstract H^{α}. Promotion of MgO with alkaline

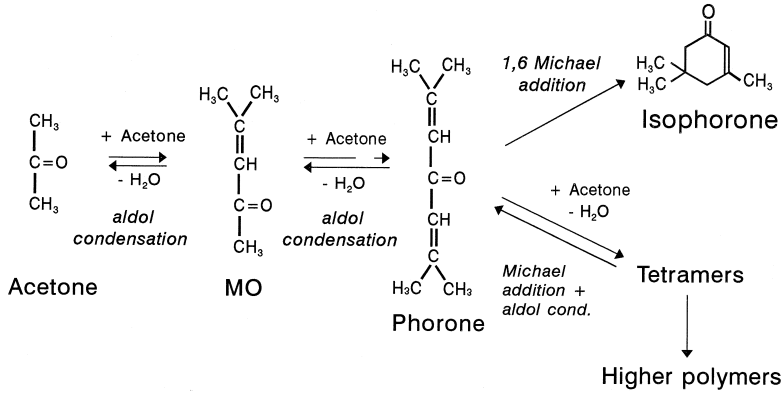

Fig. 6. Simplified reaction network for isophorone synthesis from the acetone oligomerization over basic catalysts.

metal ions increases the concentration of surface basic sites (Table 1) and enhances the MgO capacity to abstract the α-proton. As a consequence, the A/MgO samples are more active than unpromoted MgO.

In agreement with reaction mechanism in Fig. 6, Fig. 3 gives evidence for the consecutive formation of IP from MO. However, the rearrengement pathway leading from MO to cyclic IP is not straightforward since the aldol condensation between MO and a third acetone molecule may form three non-cyclic trimeric intermediates: 2,6-dimethylhepta-2,5-dien-4-one (phorone), 4,6-dimethylhepta-3,5-dien-2-one and 4,4′-dimethylhepta-2,6-dione [13]. In our experiments, phorone was the only trimeric compound detected among reaction products. Phorone is formed by deprotonation of MO in α-position to the carbonyl function and further condensation with a third acetone molecule. The lack of evidence for the presence of the other two trimers is in line with previous work by Reichle [12] who postulated that phorone is the exclusive intermediate between MO and IP. On the other hand, our catalytic results suggested that IP did not undergo, at least to any significant extent, further aldol condensation with a fourth acetone molecule to give isoxylitones, $C_{12}H_{18}O$, since heavy condensation products were detected only occasionally and in trace amounts at the beginning of the catalytic tests. This is consistent with prior results showing that formation of cyclic IP is irreversible [14] and that IP is a stable terminal product [12].

4.2. Reaction network and catalyst deactivation

The activity of unpromoted MgO and alkali-promoted MgO samples declined throughout the course of the 10 h runs. Following the catalytic tests, the spent catalysts appeared dark brown suggesting the formation of significant amounts of coke on the catalyst surface. Catalytic tests performed at different contact times on magnesium oxide showed that, contrarily to IP formation, the initial catalyst deactivation diminishes at higher contact times (Fig. 3). The fact that d_0 decreases when the IP formation increases, reveals that IP is not the species responsible for catalyst deactivation. Based on a similar interpretation, we can also discard that the MgO activity decay was caused by the presence of water in the products. In fact, synthesis of isophorone involves the concomitant formation of two water molecules while only one molecule of water is produced in the MO synthesis (Fig. 6). The partial pressure of water over the catalyst should therefore increase with increasing W/F^0 which is the opposite trend observed in Fig. 3 between d_0 and W/F^0.

Fig. 3 actually illustrates that d_0 increases when S_{MO} increases. Nevertheless, previous work has shown that MO itself is not a strong coking agent. In fact, Reichle [12], by pulsing pure MO on MgO-based catalysts, did not observe the formation of non-volatile compounds, even though MO was almost completely converted. To account for this result that relates d_0 to S_{MO} it is reasonably, therefore, to assume that coke is formed from the highly unsaturated trimeric compounds produced by aldol condensation of MO with a third molecule of acetone. As stated above, three different non-cyclic trimers are likely to be formed through the tri-oligomerization of acetone. However, we only detected phorone among reaction products, in concentrations lower than 2%. That only negligible amounts of non-cyclic trimers were present in the gaseous products would indicate that these compounds remain mostly bound to the catalyst surface, probably via their carbonyl groups. The strong adsorption of phorone on MgO catalysts and its subsequent condensation yielding higher non-volatile oligomeric compounds have been proved by Reichle [12]. The aldol or Michael addition of acetone to one of the non-cyclic trimers produces condensation products (the tetramers in Fig. 6) with a molecular mass of 178. In general, chain growth of acetone by aldol coupling on MgO-based catalysts occurs by interaction of the carbonyl oxygen with a weak Lewis acid site and interaction

of the α-proton with a strong Lewis base site. As a consequence of these interactions, electron acceptor and electron donor centers are created in the adsorbed molecule. The molecules with higher molecular mass and many oxygen-containing groups remain then adsorbed on the surface due to their stronger intermolecular electron donor–electron acceptor interactions.

We therefore conclude that MgO-based catalysts apparently deactivated due to a blockage of basic sites by heavy oligomeric compounds formed from aldol condensation of non-cyclic trimers with acetone. At low contact times, the selectivity to the primary product (MO) increases which favors the aldol condensation synthesis of non-cyclic trimers causing a rapid activity decline. At high contact times, formation of large amounts of isophorone diminishes the concentration of the phorone intermediate on the catalyst surface, thereby lowering the deactivation rate.

4.3. Catalyst deactivation and surface base property

Fig. 4 shows that the A/MgO samples deactivated faster than unpromoted MgO, following the sequence $Li < Na < K < Cs$, which coincides with the basicity order of the Periodic Table. On the other hand, for the A/MgO series a good correlation was observed between d_0 and parameter M (Fig. 5). In Table 1 it is observed that M increases when q_0, the value of the partial negative charge of oxygen in the A_xO promoter, increases. The q_0 values of the different A_xO promoter oxides can be estimated from the electronegativity equalization principle [17] and taken as a measure of the basicity of a given single-component oxide if we accept that the basicity of an oxide surface is related to the electron donor capacity of the combined oxygen anion. Thus, our results in Fig. 5 and Table 1 indicate that M, and consequently d_0, increase when the basicity of the A_xO oxide in A/MgO catalysts increases: the higher the electrodonating ability of the promoter oxide, the higher both the generation of new basic centers per mole of promoter A and the initial catalyst deactivation. This result, that relates catalyst deactivation with catalyst basicity, is interpreted by considering that promotion of MgO with alkaline metals enhances the interaction of non-cyclic trimers with the solid surface, and favors the H^{α} abstraction from the acetone molecule. As a consequence, the aldol-type condensation reactions between non-cyclic trimers and acetone that form tetramers and heavier polymers are favored which results in an increasing coke formation.

5. Conclusions

The magnesium oxide activity declines in the base-catalyzed oligomerization of acetone due to a blockage of basic sites by a carbonaceous residue created by oligomerization side reactions. The activity decay is faster when the selectivity toward the primary product (mesityl oxide) is higher compared to that of isophorone which is the cyclic terminal product. Non-cyclic trimers, such as phorone, formed from aldol condensation of mesityl oxide and acetone, are key intermediate species in coke formation. These highly unsaturated trimeric compounds remain adsorbed on the catalyst surface and yield non-volatile oligomeric compounds which block basic active sites.

Promotion of magnesium oxide with alkaline metals increases catalyst deactivation following the basicity order of the promoter oxide: the stronger the electron-donor properties of the promoter oxide, the higher the catalyst activity decline. Enhancement of the magnesium oxide basicity by alkali addition strengthens the interaction between the solid surface and the non-cyclic trimers, and improves the catalyst ability for abstracting H^{α} from the acetone molecule, thereby favoring the aldol-type condensation synthesis of tetramers and heavier polymers.

Acknowledgements

Support of this work by the Consejo Nacional de Investigaciones Científicas y Técnicas (CONICET), Argentina, the Universidad Nacional del Litoral, Santa Fe, Argentina, and the Japan International Cooperation Agency (JICA) is gratefully acknowledged.

References

[1] S. Malinovski, M. Marczewski, Catalysis, R. Soc. Chem. 8 (1989) 107.
[2] K. Tanabe, M. Misono, Y. Ono, H. Hattori, Stud. Surf. Sci. Catal. 51 (1989) 327.
[3] J.S. Lee, S.T. Oyama, Catal. Rev. Sci. Eng. 30 (1988) 249.
[4] Y. Amenomiya, V.I. Birss, M. Goledzinowski, J. Galuszka, A.R. Sanger, Catal. Rev. Sci. Eng. 32 (1990) 163.
[5] H. Hattori, in: M. Che, G.C. Bond (Eds.), Adsorption and Catalysis on Oxide Surfaces, Elsevier, Amsterdam, 1985, p. 319.
[6] G. Zhang, H. Hattori, K. Tanabe, Appl. Catal. 36 (1988) 198.
[7] K. Tanabe, G. Zhang, H. Hattori, Appl. Catal. 48 (1989) 63.
[8] M. Ai, in: L. Guczi et al. (Eds.), New Frontiers in Catalysis, Elsevier, Amsterdam, 1993, p. 1199.
[9] H. Kurokawa, T. Kato, T. Kuwabara, W. Ueda, Y. Morikawa, Y. Moro-Oka, T. Ikawa, J. Catal. 126 (1990) 208.
[10] J.I. Di Cosimo, V.K. Díez, C.R. Apesteguía, Appl. Catal. 137 (1) (1996) 149.
[11] J.I. Di Cosimo, C.R. Apesteguía, J. Molec. Catal. 91 (1994) 369.
[12] W.T. Reichle, J. Catal. 63 (1980) 295.
[13] G.S. Salvapati, K.V. Ramanamurty, M. Janardarano, J. Mol. Catal. 54 (1989) 9.
[14] S. Lippert, W. Baumann, K. Thomke, J. Mol. Catal. 69 (1991) 199.
[15] C.D. Chang, A.J. Silvestri, J. Catal. 47 (1977) 249.
[16] C.O. Veloso, J.L.F. Monteiro, E.F. Sousa-Aguiar, in: J. Weitkamp, H.G. Karge, H. Pfeifer, W. Hölderich (Eds.), Zeolites and Related Microporous Materials: State of Art 1994, Elsevier, 1994, p. 1913.
[17] R.T. Sanderson, Chemical bonds and bond energy, 2nd ed., Academic Press, New York, 1976.